Multiframe Visual-Inertial Blur Estimation and Removal for Unmodified Smartphones (Supplementary Material)

Gábor Sörös, Severin Münger, Carlo Beltrame, Luc Humair
Department of Computer Science
ETH Zurich
soeroesg@ethz.ch, {muengers|becarlo|humairl}@student.ethz.ch

1 DERIVATION OF MULTIFRAME NON-BLIND BLUR REMOVAL

1.1 Original algorithm

The fast non-blind uniform blur removal algorithm of Krishnan and Fergus [Kri09] minimizes the following energy function:

$$\min_{\mathbf{x}} \sum_{i=1}^{N} \left(\frac{\lambda}{2} (\mathbf{x} * \mathbf{k} - \mathbf{y})_i^2 + \sum_{j=1}^{J} |(\mathbf{x} * \mathbf{f_j})_i|^{\alpha} \right) \tag{1}$$

where $f_x = [1 \ -1]$ and $f_y = [1 \ -1]^T$ denote differential operators in horizontal and vertical directions, respectively. λ is a factor to balance the error function and the prior term. For brevity, the notation $F_i^d \mathbf{x} := (\mathbf{x} * f_d)_i$ and $K_i \mathbf{x} := (\mathbf{x} * \mathbf{k})_i$ will be used in the following formulas. Applying the half-quadratic penalty method of Geman [Gem95], we can introduce auxiliary variables w_i^x and w_i^y, together denoted as $\mathbf{w}$, to split the energy function into a quadratic problem in $\mathbf{x}$ and a pixel-wise problem in $\mathbf{w}$, and solve for $\mathbf{x}$ and $\mathbf{w}$ iteratively by fixing the other variable.

$$\min_{\mathbf{x},\mathbf{w}} \sum_{i} \left(\frac{\lambda}{2} (\mathbf{x} * \mathbf{k} - \mathbf{y})_i^2 + \frac{\beta}{2} (\|F_i^1 \mathbf{x} - w_i^1\|_2^2 + \|F_i^2 \mathbf{x} - w_i^2\|_2^2) + |w_i^1|^{\alpha} + |w_i^2|^{\alpha} \right) \tag{2}$$

The solution of the $\mathbf{x}$-subproblem given fixed $\mathbf{w}$ can be efficiently calculated using Fast Fourier Transforms because in the frequency domain convolutions become multiplications. Deriving the above equation w.r.t. $\mathbf{x}$ and setting the derivative to zero:

$$\left(F^{1^T} F^1 + F^{2^T} F^2 + \frac{\lambda}{\beta} K^T K \right) \mathbf{x} = F^{1^T} \mathbf{w}^1 + F^{2^T} \mathbf{w}^2 + \frac{\lambda}{\beta} K^T \mathbf{y} \tag{3}$$

from which we get $\mathbf{x}$:

$$\mathbf{x} = \mathscr{F}^{-1} \left(\frac{\mathscr{F}(F^1)^* \circ \mathscr{F}(\mathbf{w}^1) + \mathscr{F}(F^2)^* \circ \mathscr{F}(\mathbf{w}^2) + (\lambda/\beta) \mathscr{F}(K)^* \circ \mathscr{F}(\mathbf{y})}{\mathscr{F}(F^1)^* \circ \mathscr{F}(F^1) + \mathscr{F}(F^2)^* \circ \mathscr{F}(F^2) + (\lambda/\beta) \mathscr{F}(K)^* \circ \mathscr{F}(K)} \right) \tag{4}$$

where $*$ denotes complex conjugate, and multiplications and divisions are performed element-wise.

The solution of the $\mathbf{w}$-subproblem is obtained by solving $2N$ (N is the number of pixels in the image) independent 1D problems of the form

$$\arg\min_{w} |w|^{\alpha} + \frac{\beta}{2} (w - F_i^d \mathbf{I})^2 \qquad (F_i^d \in \{F_i^x, F_i^y\}) \tag{5}$$

For $\alpha = \frac{1}{2}, \alpha = \frac{2}{3}$ and $\alpha = 1$ even an analytical solution is given, for other values a Newton-Raphson root finder method can be applied [Kri09].

1.2 Our extension

We extend the above algorithm with a new penalty term that incorporates information from other images of the same scene. Specifically, we added a new penalty term which describes a weighted squared difference of the latent image patch $\mathbf{x}$ from M other patches $\mathbf{x}_j, j \in 1 \dots M$ that are estimated from blurry image patches $\mathbf{y}_j$. The weights μ_j are chosen inversely proportional to the 'blurriness' of the corresponding blurry image patch $\mathbf{y}_j$. We assume the rolling-shutter distortion has already been compensated in the input images.

We give here the solution of the $\mathbf{x}$-subproblem with one additional input image patch. Let us denote our blurry image patch with $\mathbf{y}$, our additional blurry image patch with $\mathbf{y}_2$, and the whole images as $\mathbf{B}$ and $\mathbf{B}_2$, respectively. We first perform single-frame patch-wise uniform deconvolution on $\mathbf{B}_2$ as described in Section 4 of the paper to get a sharpened image $\tilde{\mathbf{X}}_2$. Then, we align $\tilde{\mathbf{X}}_2$ with $\mathbf{B}$ to get $\tilde{\mathbf{X}}'_2$. An aligned and sharpened patch in $\tilde{\mathbf{X}}'_2$ corresponding to $\mathbf{y}_2$ is denoted as $\tilde{\mathbf{x}}'_2$. After image alignment, we minimize the following energy function:

$$\min_{\mathbf{x}} \sum_{i=1}^{N} \left(\frac{\lambda}{2} (\mathbf{x} * \mathbf{k} - \mathbf{y})_i^2 + \frac{\mu}{2} (\mathbf{x} - \tilde{\mathbf{x}}'_2)_i^2 + \sum_{j=1}^{J} |(\mathbf{x} * \mathbf{f_j})_i|^\alpha \right) \tag{6}$$

Again, by applying the half-quadratic splitting method we transform our problem into an $\mathbf{x}$-subproblem and a $\mathbf{w}$-subproblem.

$$\min_{\mathbf{x},\mathbf{w}} \sum_i \left(\frac{\lambda}{2} (\mathbf{x} * \mathbf{k} - \mathbf{y})_i^2 + \frac{\mu}{2} (\mathbf{x} - \tilde{\mathbf{x}}'_2)_i^2 + \frac{\beta}{2} (\|F_i^1 \mathbf{x} - w_i^1\|_2^2 + \|F_i^2 \mathbf{x} - w_i^2\|_2^2) + |w_i^1|^\alpha + |w_i^2|^\alpha \right) \tag{7}$$

Here $\frac{\mu}{2}(\mathbf{x} - \tilde{\mathbf{x}}'_2)_i^2$ is in matrix form

$$\frac{\mu}{2} (\mathbf{x} - \tilde{\mathbf{x}}'_2)^T (\mathbf{x} - \tilde{\mathbf{x}}'_2) = \frac{\mu}{2} (\mathbf{x}^T \mathbf{x} - 2\mathbf{x}^T \tilde{\mathbf{x}}'_2 + \tilde{\mathbf{x}}_2'^T \tilde{\mathbf{x}}'_2) \tag{8}$$

and its derivative w.r.t $\mathbf{x}$ is

$$\frac{\mu}{2} (2\mathbf{x} - 2\tilde{\mathbf{x}}'_2) = \mu (\mathbf{x} - \tilde{\mathbf{x}}'_2) \tag{9}$$

The solution of the x-subproblem given fixed $\mathbf{w}$ is calculated in the frequency domain. Deriving equation 7 w.r.t. $\mathbf{x}$, plugging in the derivative of our new prior term, and setting the derivative to zero we get

$$\left(F^{1^T} F^1 + F^{2^T} F^2 + \frac{\lambda}{\beta} K^T K + \frac{\mu}{\beta} \Delta^T \Delta \right) \mathbf{x} = F^{1^T} \mathbf{w}^1 + F^{2^T} \mathbf{w}^2 + \frac{\lambda}{\beta} K^T \mathbf{y} + \frac{\mu}{\beta} \Delta^T \tilde{\mathbf{x}}'_2 \tag{10}$$

where $F^i \mathbf{x} = \mathbf{x} * f_i$, $K\mathbf{x} = \mathbf{x} * \mathbf{k}$, and $\Delta \mathbf{x} = \mathbf{x} * \delta$ is a convolution with the Dirac delta kernel (identity). From this we can get x:

$$\mathbf{x} = \mathscr{F}^{-1} \left(\frac{\mathscr{F}(F^1)^* \circ \mathscr{F}(\mathbf{w}^1) + \mathscr{F}(F^2)^* \circ \mathscr{F}(\mathbf{w}^2) + (\lambda/\beta) \mathscr{F}(K)^* \circ \mathscr{F}(\mathbf{y}) + (\mu/\beta) \mathscr{F}(\Delta)^* \circ \mathscr{F}(\tilde{\mathbf{x}}'_2)}{\mathscr{F}(F^1)^* \circ \mathscr{F}(F^1) + \mathscr{F}(F^2)^* \circ \mathscr{F}(F^2) + (\lambda/\beta) \mathscr{F}(K)^* \circ \mathscr{F}(K) + (\mu/\beta) \mathscr{F}(\Delta)^* \circ \mathscr{F}(\Delta)} \right) \tag{11}$$

Since δ is the identity kernel of convolution, its Fourier transform $\mathscr{F}(\Delta)$ is a matrix of ones and our formula simplifies to

$$\mathbf{x} = \mathscr{F}^{-1} \left(\frac{\mathscr{F}(F^1)^* \circ \mathscr{F}(\mathbf{w}^1) + \mathscr{F}(F^2)^* \circ \mathscr{F}(\mathbf{w}^2) + (\lambda/\beta) \mathscr{F}(K)^* \circ \mathscr{F}(\mathbf{y}) + (\mu/\beta) \mathscr{F}(\tilde{\mathbf{x}}'_2)}{\mathscr{F}(F^1)^* \circ \mathscr{F}(F^1) + \mathscr{F}(F^2)^* \circ \mathscr{F}(F^2) + (\lambda/\beta) \mathscr{F}(K)^* \circ \mathscr{F}(K) + (\mu/\beta) \mathscr{F}(\Delta)} \right) \tag{12}$$

We can generalize the above solution to $1 \le j \le M$ additional images:

$$\mathbf{x} = \mathscr{F}^{-1} \left(\frac{\mathscr{F}(F^1)^* \circ \mathscr{F}(\mathbf{w}^1) + \mathscr{F}(F^2)^* \circ \mathscr{F}(\mathbf{w}^2) + (\lambda/\beta) \mathscr{F}(K)^* \circ \mathscr{F}(\mathbf{y}) + \frac{\mu}{\beta \sum_j \mu_j} \mathscr{F}(\sum_j \mu_j \tilde{\mathbf{x}}'_j)}{\mathscr{F}(F^1)^* \circ \mathscr{F}(F^1) + \mathscr{F}(F^2)^* \circ \mathscr{F}(F^2) + (\lambda/\beta) \mathscr{F}(K)^* \circ \mathscr{F}(K) + (\mu/\beta) \mathscr{F}(\Delta)} \right) \tag{13}$$

The solution of the $\mathbf{w}$-subproblem is analog to the original algorithm.

2 ADDITIONAL RESULTS OF REMOVING SYNTHETIC BLUR

2.1 Comparison of deconvolution methods

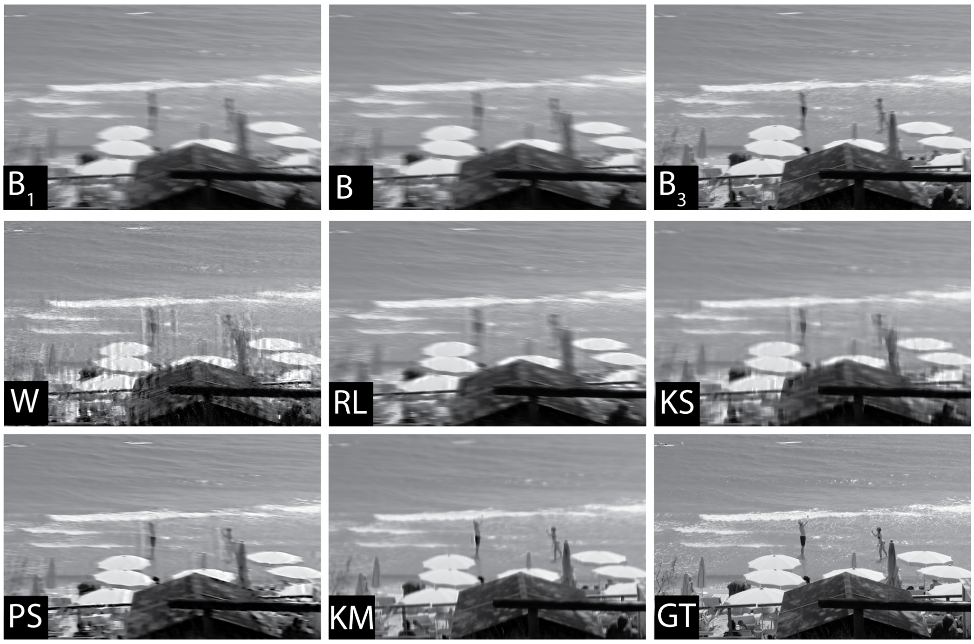

Figure 1: This figure contains all results of the quantitative experiment shown in Table 1 in the paper. B is the input image for patch-wise uniform deconvolution using the gyro-generated kernels and with different deconvolution methods: Wiener filter (W), Richardson-Lucy algorithm (RL), Krishnan's algorithm (KS). For comparison, we also show the output of Photoshop's ShakeReduction feature (PS) which is a blind uniform deconvolution method (i.e., a single blur kernel is estimated from the image content only). The result of our multi-frame deconvolution using B_1 and B_3 as additional priors is shown in the middle column in the bottom row (KM). The ground truth is shown in GT.

2.2 Beach example

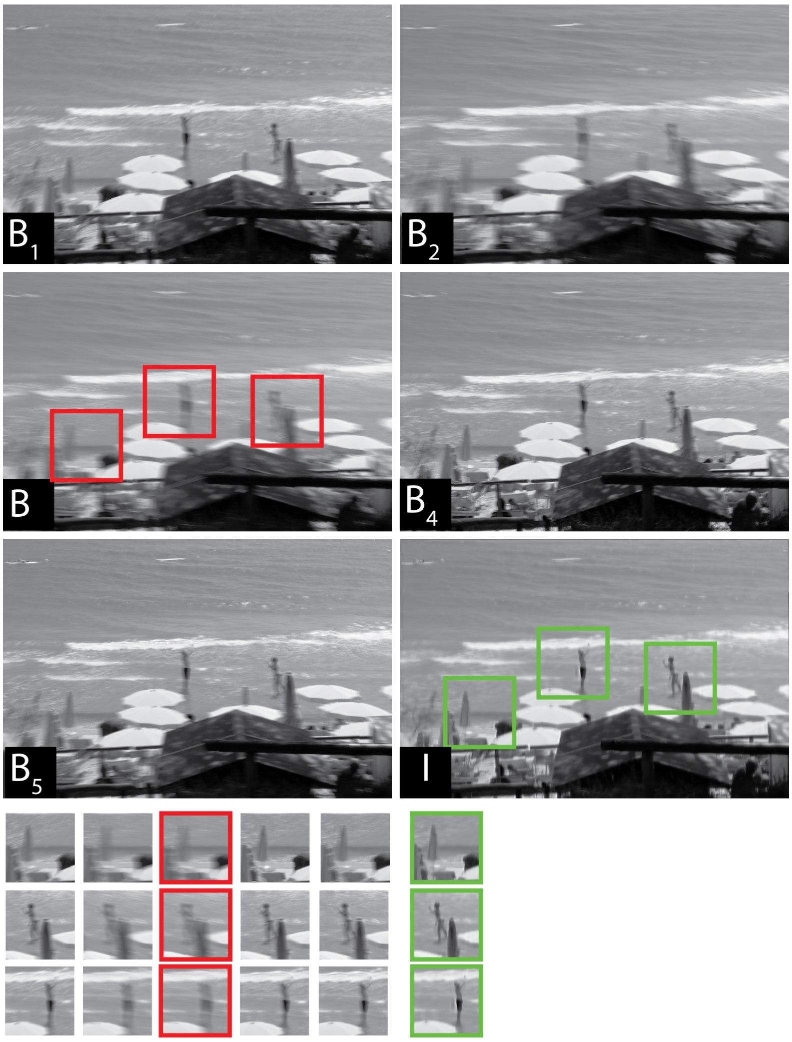

Figure 2: Removing synthetic blur (all images of the synthetic blur example in the paper). B is the main input image and $B_{1,2,4,5}$ neighboring images aid the blur removal, I is our result. Bottom: corresponding patches from the 5 input images and the result.

2.3 House example

In this example, we synthetically generated 5 blurry images B_1–B_5 and deblurred $B = B_3$ using $B_{1,2,4,5}$ as additonal priors in our multiframe deblurring algorithm. The final result is shown in I. In the following pages we also show the estimated kernels and the intermediate single-frame deblurring results.

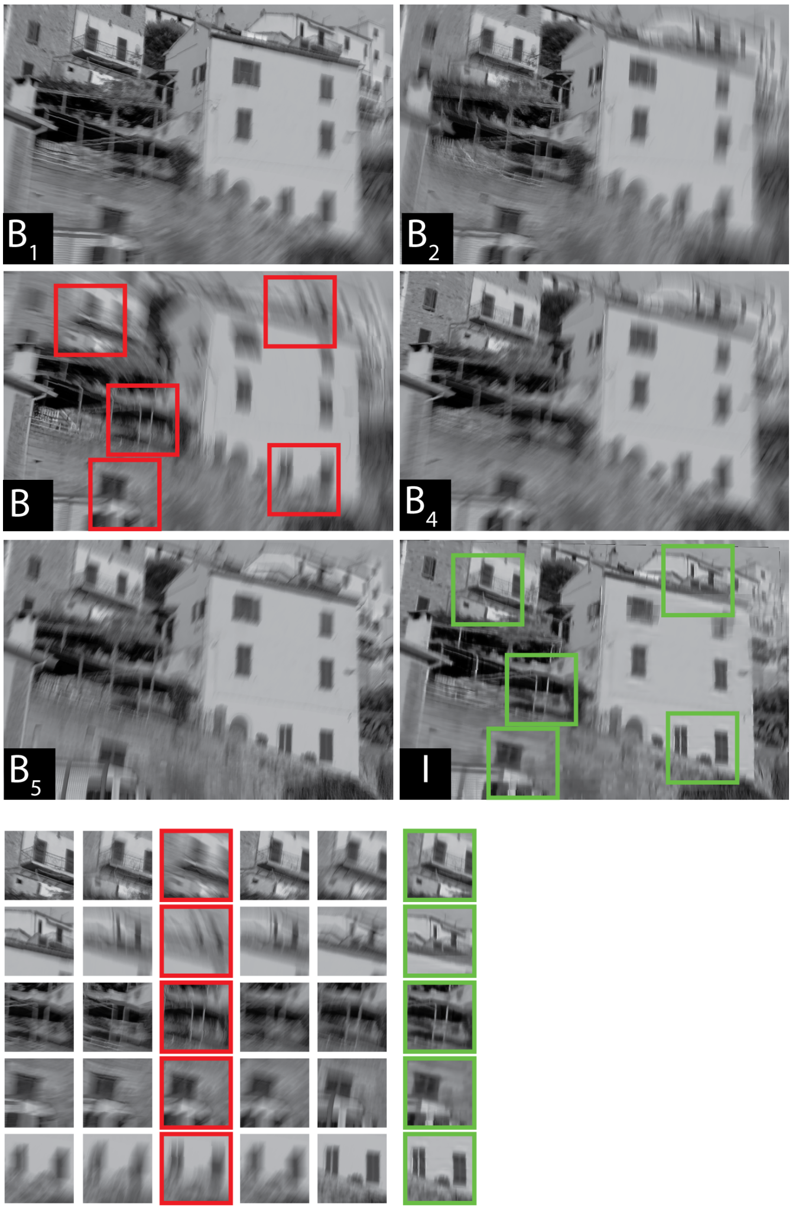

Figure 3: Removing synthetic blur. B is the main input image and $B_{1,2,4,5}$ neighboring images aid the blur removal, I is our result. Bottom: corresponding patches from the 5 input images and the result.

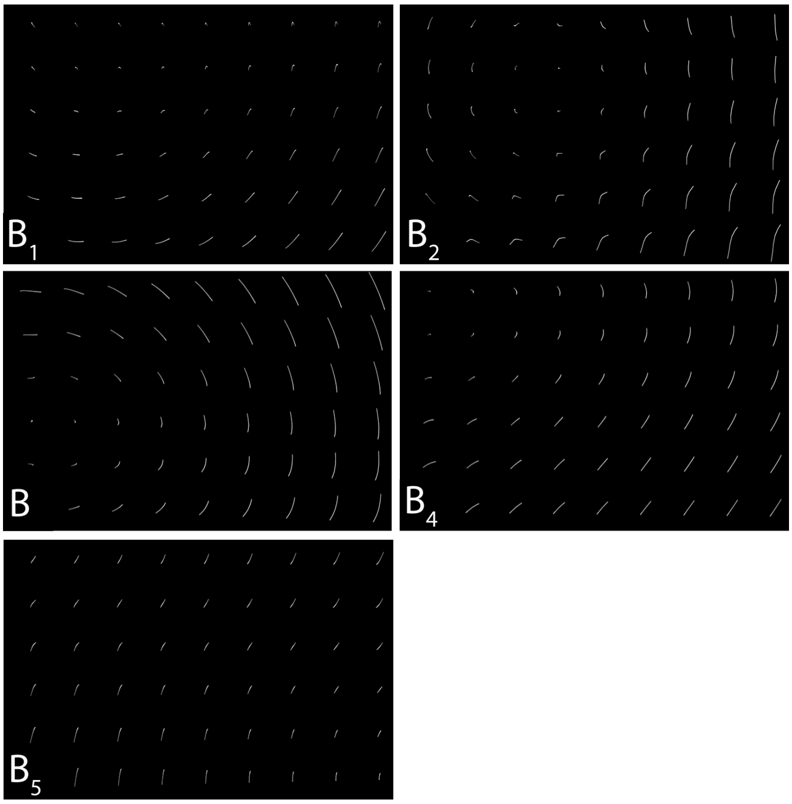

Figure 4: The blur kernels estimated from gyroscope data for the house example (Figure 3)

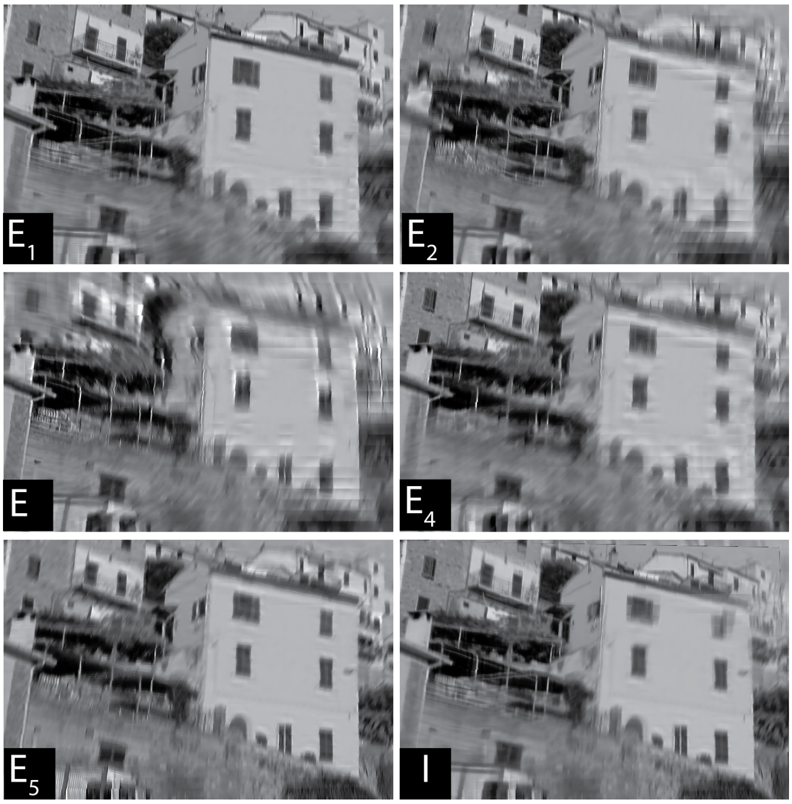

Figure 5: The intermediate deblurred single frames E_1–E_5 for the house example (Figure 3) and our multi-frame deblurred result I. Single-frame deblurring often fails in areas with large blur, hence the individual E images are of low quality. Information from multiple (differently blurred) images clearly improves the quality of the overall restoration (c.f. B and I of the example).

3 ADDITIONAL RESULTS OF REMOVING REAL BLUR

3.1 Sign example

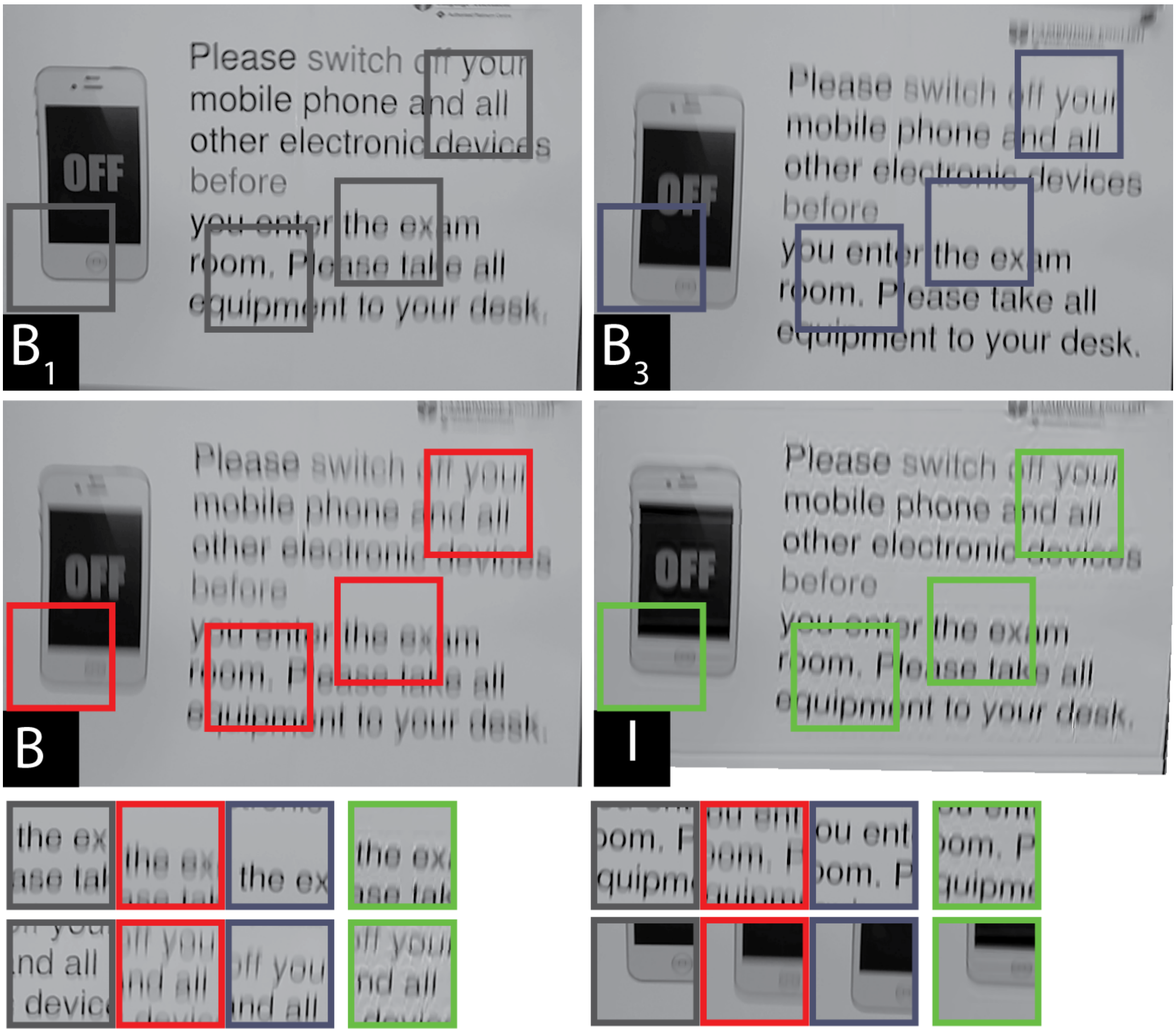

Figure 6: Restoring B with the help of $B_{1,3}$, all degraded with real motion blur. (The sign example from the paper in high resolution.)

3.2 Books example

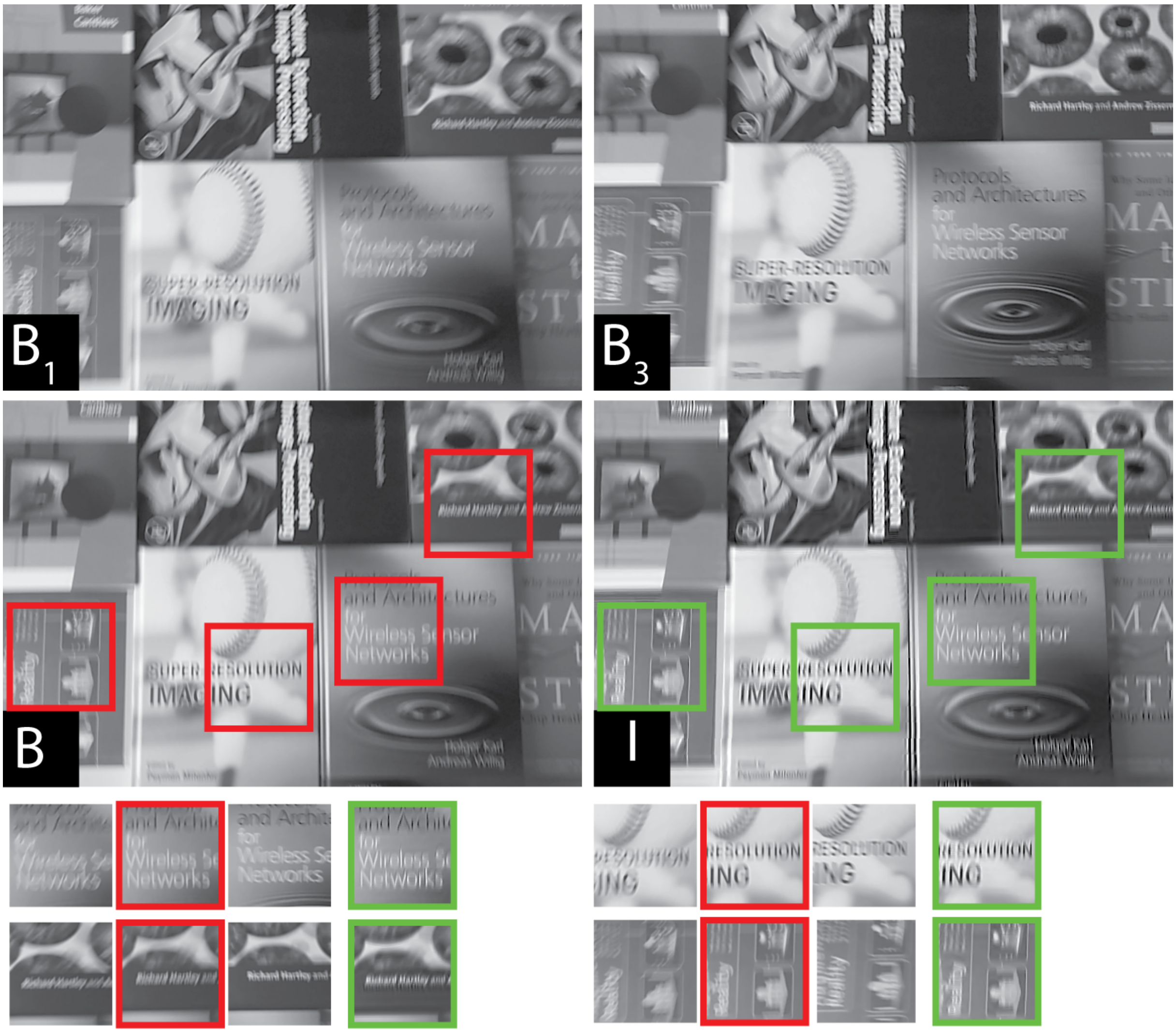

Figure 7: Restoring B with the help of $B_{1,3}$, all degraded with real motion blur.

3.3 Newspapers example

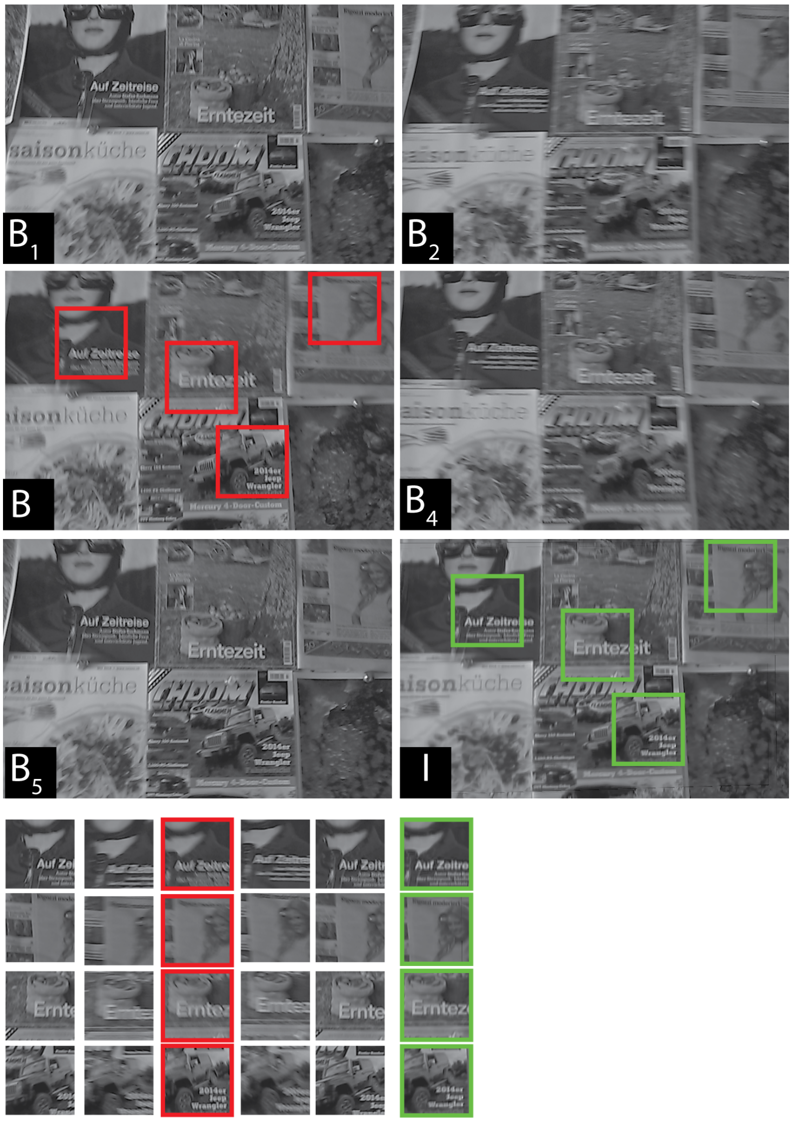

Figure 8: Restoring B with the help of $B_{1,2,4,5}$, all degraded with real motion blur. Our result is shown in the bottom right (I)

4 REFERENCES

[Kri09] D. Krishnan and R. Fergus. Fast image deconvolution using hyper-Laplacian priors. In *Advances in Neural Information Processing Systems (NIPS)*. 2009.

[Gem95] D. Geman ans Y. Chengda. Nonlinear image recovery with half-quadratic regularization. In *IEEE Transactions on Image Processing, Vol.4, No.7*. 1995.